POLITECNICO DI TORINO

Corso di Laurea Magistrale

In INGENERIA MECCANICA

Tesi di Laurea magistrale

Process and design optimization for lattice structure made by Electron Beam Melting process

Relatore

Manuela Galati

Co-Relatore

Abdollah Saboori

Giovanni Rizza

Candidato

Augusto Chávez

Anno Academico 2020/2021

Contents

List of figures

List of tables

Abstract

Titanium aluminide are intermetallic materials used for lightweight and high temperature application, especially in the aerospace and automotive industry. Recently also it started to be considered as an alternative material for implants in the medical sector. The processability of titanium aluminide present many challenges because of the lack of ductility at room temperature. Additive manufacturing techniques, in particular, electron beam melting (EBM) emerge as suitable solution for the manufacture of different components made of this material. Up to now, few studies have been carried out in order to address the manufacturing challenges and describe the mechanical properties of titanium aluminide components manufactured via additive manufacturing. A review of the state of the art of the processability and characteristics of titanium aluminide is presented in this paper. In the experimental part of the project fourteen different lattice structures samples where produced. The correct fabrication and mechanical characteristic of this samples were analyzed by compression test.

1. Introduction

Titanium aluminide (TiAl) are intermetallic materials in which the main two components are titanium and aluminum [1]. Among all, the most used for engineering applications is the Ti-48Al-2Cr-2Nb[2]. TiAl materials exhibit good corrosion and creep resistance combined with low density and good mechanical strength [1]. The final mechanical properties of a component manufactured of titanium aluminide depends not only on the chemical composition but also on the obtained microstructure. Because of the previous mentioned properties, titanium aluminide are used in the aerospace industry in the manufacture of gas turbines blades, nozzles, exhaust components and lightweight structures as a replacement of other heaver materials like nickel superalloys [1] [3][4][2]. The automotive industry also benefits of the characteristics of this materials in the manufacture of high performance turbochargers and exhaust valves [5][6][7] [2]. The medical sector recognize the potential of titanium aluminide as for implants application, for that reason, recently, several studies have been carried out to demonstrate the biocompatibility of titanium aluminide in other to use it for bone implants as an alternative to other titanium alloys like Ti-6Al-4V [8][9][10][11].

Traditionally, titanium aluminide components were manufactured using casting techniques whit a hot post processing like HIP in order to reduce the crack formations and powder metallurgy (PM) [12][13]. The low ductility and toughness at room temperature make difficult the machinability of titanium aluminide [14]. In order to overcome this issues, additive manufacturing techniques like electron beam melting (EBM), laser powder bed fusion (LPBF) and direct energy deposition (DED) have been considered as a suitable solution for the manufacture of TiAl components [13]. These technologies allow to manufacture component, by introducing a hot process like in the case of EBM, that allow to manufacture at temperature above the ductile to brittle transformation temperature [14]. Another important aspect is the economical, in this case additive manufacturing techniques allows the production of

component whit less material usage, and allowing the production of small batch of components[15]

Additive manufacturing (AM) is defined by ASTM as a “process of joining materials to make objects from 3D model data, usually layer upon layer”[16]. AM process can be classified in binder jetting, direct energy deposition, material extrusion, material jetting, powder bed fusion, vat photopolymerization and sheet lamination [16]. The additive manufacturing techniques suitable for metallic components are powder bed fusion (PBF), that can be subdivided into laser powder bed fusion (LPBF) and electron beam melting (EBM), and direct energy deposition that can be subclassified in electron beam free-form (EBF), direct laser fabrication (DLF), direct metal deposition (DMD) and wire arc additive manufacturing (WAAM) [17].

Several studies were carried out to describe the processability of titanium aluminide via additive manufacturing. Murr et al. [2] characterized the microstructure of samples manufactured via EMB. Ge et al[18] characterized the chemical composition of the final component according to the build parameters using EBM. Baudana et al. [6] performed mechanical test in bulk samples at room and high temperatures. Seifi et al. [19] compared the defect distribution and mechanical properties of EBM manufactured bulk samples. Todai et al. [20] studied the tensile properties of bulk specimens manufactured by electron beam melting. Youn et al. [21] investigate on the microstructure and compressive behavior of samples manufactured via EBM. Mohammad el al. [22] performed mechanical test on lattice structures samples manufactured by EBM. Lin et al. [23] tested EBM manufactured samples to analyze the anisotropy of microstructure and tensile properties.

Currently there are not many studies that describe the mechanical properties of titanium aluminides components manufactured by additive manufacturing techniques. The aim of the current paper is to review the state of the art of the potential, challenges, and feasible solution of additive manufacturing for titanium aluminides components with an emphasis on electron beam melting manufactured lattice structures.

2. Titanium aluminides (TiAl)

2.1. Properties

Intermetallic materials that have been developed for high temperature applications as a replacement for superalloys. Even if they show good properties, the fact that they exhibit extreme brittleness limited it application. The increase in the utilization of powder metallurgy increased the use of this materials for the fabrication of complex shapes and high-performance components. Titanium aluminide (TiAl) are intermetallic materials, in which the main two elements are titanium and aluminum. [1].

TiAl materials have desirables characteristics for designers and engineers like good creep and oxidation resistance, low density, high strength, that are optimal for lightweight structures, and components that operates at high temperature [1]. Comparing it with others titanium

alloys like the Ti-6Al-4V, titanium aluminide materials have lower ductility and fracture toughness at room temperature, and lower strength, but it is also lighter. The factors mentioned before where the main reason why engineers use to avoid this materials for a greater variety of components, and where only used in high performance applications[12]. Another disadvantage pointed out in the literature is the low the wear resistance when exposed to high friction (for example in internal combustion engine pistons), but this can be solve using metal coatings [24].

For high temperature application, the main competitor for the TiAl is the nickel superalloy which is a material two times heavier, but that have better ductility at room temperature and is at least 65 times cheaper to manufacture, that leads to the use of TiAl components only when is strictly needed [12].

2.2. Microstructure and chemical composition

The properties of titanium aluminide materials are strongly related to the microstructure, which is affected by the manufacturing process and heat treatments performed on the component. Four types of microstructures can be obtained: fully lamellar, nearly lamellar, duplex and equiaxial near-γ. If the desired characteristics includes good fatigue resistance, fracture toughness and creep resistance, a fully lamellar microstructure is the better alternative. By means of traditional manufacturing techniques like casting and forging is not possible to control the final microstructure obtained. In the other hand, EBM technology allows the control of the microstructure during the manufacturing process because it melts layer by layer the powder and maintain the surrounding of the melting pool at an optimal temperature. In the case of titanium aluminide, in other to obtain good creep and oxidation resistance, the building temperature should be above the ductile to brittle transformation temperature that is around 800° C [18][20].

According to the percentage of aluminum, titanium aluminides can be categorize in three different phases, Ti_3Al (α_2), TiAl (γ) and $TiAl_3$ from which only first two, and a dual phase from both have been used in engineering applications [12]. Good high temperature strength and low ductility have been found in Ti_3Al (aluminum content in the rage of 22% to 39%), but it exhibits brittleness. The γ phase that have aluminum in a 48% to 66% have good corrosion resistance, but at room temperature, its ductility is null. In order to achieve better mechanical properties like high strength at room and high temperature, as well as good ductility, dual phases material made of a mixture of Ti_3Al (α_2) and TiAl (γ) have been developed. The aluminum content in dual phase titanium aluminide can go from 40% up to 48% [12]. Normally titanium aluminide materials suitable for engineering application have 42% to 49% of aluminum, and 0.1 % to 10% of other elements like Nb, Cr, V, Ta, Mo and Zr. The final chemical composition varies according to the desired phases and mechanical characteristics of the component to be manufactured, but in general the most used is the Ti-48Al-2Cr-2Nb [25].

2.3. Applications

Because of new manufacturing techniques like EBM and their mechanical characteristic, the use of titanium aluminide components in the industry is increasing.

In the aerospace industry is used nowadays as an alternative to heavier nickel base superalloys in turbine blades. The use of TiAl manufactured using EBM technology turbine blades for the 6^{th} and 7^{th} stages of the low-pressure turbine of the General Electric GEnx aircraft engine allows a reduction of weight of 400 lb. and contributes to the increase of fuel efficiency and CO2 emission up to 15% comparing it with previous generation engines [3][26].

In the automotive sector is used to manufacture exhaust valves, turbochargers wheels, pistons and other components, especially for high performance applications [5][12]. Mitsubishi Motor Corp introduced in 1999 a casting manufactured titanium aluminide turbocharger for the Lancer Evolution VI car (street version and rally version), this improves the performance through a reduction of weight in comparison with previous versions [5].

Because of its low density and good mechanical properties compared to other materials used for orthopedic implants, researcher in the medical field considered as potential material. Apart of that, been a Vanadium-free make it more attractive, because recent studies found that Vanadium-ion can be generated in Ti-6Al-4V implants, and that it can leak to the blood vessel, being potentially hazardous for the human body [27] [22].

In the medical field, the use of additive manufacturing techniques has proven to be a success because it facilitates the manufacture customized orthopedic implants with better finishing than the ones manufactured with traditional manufacturing techniques and the use of materials like titanium aluminides. Furthermore, it allows the use of lattice structures of different kind in order to obtain an implant whose mechanical properties are similar to the human bones [28].

Regarding the biocompatibility of the gamma titanium aluminide as a biomaterial for orthopedic implants, many research activities have been done. Santiago-Medina et al. [8] compared the through an in-vitro experiment the biocompatibility of Ti-6Al-4V and Ti-48Al-2Cr-2Nb disks. To improve the cellular activities, a layer of TiO_2have been added to the samples by means of a micro arc oxidation process. Good cell adhesion has been found at the end of the experiments. In another work, Mohammad et al. [9] compared the wear resistance of EBM-manufactured TiAl hipped samples and pure titanium samples. The results showed that the TiAl samples exhibit better corrosion resistance in an in-vitro experiment. Bello et al. [10] suggest in their wok that thermally oxidized showed good cell adhesion and proliferation. Castañeda-Muñoz et al. [11] made in-vivo experiments of Ti-48Al-2Cr-2Nb cylindrical implants in rats. After 6 moth they observed good bone growth without any kind of rejection, tumors, or other adverse reaction.

2.4. Processability

Titanium aluminide component have been manufactured using casting, wrought processing, powder metallurgy and additive manufacturing techniques. As mentioned, titanium aluminide offers many desirable mechanical characteristics but also oppose many challenges to it massive application at industrial level, especially regarding the cost [12] [13].

2.4.1. Casting

Investment casting have been one of the most used manufacturing processes used to mass produce component made of titanium aluminide. In order to obtain good mechanical properties, the component should undergo a hot post processing (in the range of 1200°C to 1350°C) and because the obtained microstructure are columnar grains, that results in high anisotropy in the mechanical properties that are not easily reversible[12]. After the casting, the machinability of the components is also a challenge, due to the high hardness and brittleness. It leads to poor surface finishing and decreases the tool life [29][30][25]. The above mentioned implies that the cost associated to the machinery and energy consumption is higher in comparison whit other materials like nickel superalloys [12].

2.4.2. Wrought processing.

An alternative to overcome the anisotropy of casting technique is the wrought process. Adopting thermomechanical process above the ductile to brittle transformation temperature allow the production of component with a more homogeneous microstructure and properties. The main drawback of this process need tools that can sustain temperature above 1000 °C and neutral atmosphere [25].

2.4.3. Powder metallurgy

Powder metallurgy (PM) have been used to manufacture high quality complex component made of various metallic materials. Adopting this technique components can be manufactured at near shape, reducing the need of a machining post processing [25]. It also offered an improvement to the porosity and chemical inhomogeneity in comparison with casting. [12] [25].

The most studied process is the hot isostatic pressing, using as a raw material gas atomized pre alloyed powder. The process presses the powder using pressure in the range of 100MPa to 150MPa and temperature of 1200°C to 1400°C. The process produces homogeneous microstructure but the coarse grain size.

The main drawbacks of this techniques are that micro porosities and contamination cannot be easily removed, leading to limited mechanical properties. Also, the shrinkage of the component should be calculated and taken into consideration [12]

2.4.4. Additive manufacturing

In recent year, additive manufacturing techniques gained popularity as an alternative to produce component made of titanium aluminide materials. Complex geometries, highly

customizable component and the possibility to optimize the process parameter in order to obtain almost 100% dense component with minimum defect are the key factor that increase the research and development in this area [25]. Among all the additive manufacturing technologies available, EBM is the one that presents better results [30].

3. Metal Additive Manufacturing (AM)

Additive manufacturing (AM) is defined by ASTM as a "process of joining materials to make objects from 3D model data, usually layer upon layer"[16]. This manufacturing processes allows the fabrication of near net shape components without any restriction from the production methods. From the 3 CAD model of the component to be manufactured, the information of the geometry and process parameters are sent to the AM machine through an STL file, and the component is build up by adding thin layers of materials one on top to the other [31][7].

AM processes is been used since the seventies, firstly, they were used for rapid prototyping (RP) where components where manufactured mainly using polymers, paper, and wood material. The industry saw the potential of additive manufacturing as a tool for manufacturing final components, and not only prototypes, and the use of this technologies changed from just rapid prototyping to rapid manufacturing (RM) [17]. Because of the great amount of technologies available in the market a classification of this technologies was needed. According to ASTM, the AM process can be classified in binder jetting, direct energy deposition, material extrusion, material jetting, powder bed fusion, vat photopolymerization and sheet lamination [16].

The additive manufacturing techniques suitable for metallic components are powder bed fusion (PBF), that can be subdivided into laser powder bed fusion (LPBF) and electron beam melting (EBM), and direct energy deposition that can be subclassified in electron beam free-form (EBF), direct laser fabrication (DLF), direct metal deposition (DMD) and wire arc additive manufacturing (WAAM) [17].

For mass production of metallic components, the most used technologies are electron beam melting (EBM) and laser powder bed fusion (LPBF), both corresponding to the category of powder bed fusion [32]. Both technologies uses as a raw material powder, in the case of EMB the recommended range for the size is between 40 and 105 µm, for LPBF the range goes from 10 to 45 µm [15][31]. The main difference between the two processes is that, EBM uses as a heat source a high power electron beam, the build chamber is under vacuum, and the allows the possibility to preheat the material allowing the manufacture of final components without residual stresses [15]. On the other hand, SLS that is the most used technology up to now, uses a laser beam to melt the powder and the manufacturing process is done in an inert atmosphere. LPBF allows the processability not only of a greater amount of metallic materials comparing it with EBM, but also allows the processability of ceramic and polymers. DED, besides been used for manufacturing process, it also offers the possibility to repair metallic components, using the same principles as welding[32].

Comparing it with other manufacturing techniques like casting and machining offers complete freedom in the geometry of the final components to be manufactured, allowing to produce topology optimized components, lightweight lattice structures, optimized cooling channel, internal cuts with a good dimensional accuracy[32]. The components can also be highly customizable and because it only uses material where is needed, the waste materials can be minimal, that is an important favor when high performance material like titanium aluminide is use. Also, it does not require any preparation before starting the manufacturing process, and Finally because the component can be produced on-demand, the carbon foot print o the component can be reduced because it reduces the need to have storage facilities [7][33][31][17]. Currently the drawbacks that faces AM technologies are low productivity, the maximum size of the components that are limited to the building chamber and that component have to be built on a flat base [17].

3.1. Powder Bed Fusion (PBF)

3.1.1. Electron beam melting

EBM is a AM process than can be used to achieve component with a near 100% apparent density even with complex geometries, and is used to manufacture components made of metallic materials stainless steel, tool steel, Ni-based superalloys, Co-based superalloys, Ti-based alloys, intermetallic, aluminum, beryllium, and niobium [33]. Among all the, nowadays is used mainly for titanium base materials because it solves many problems in the manufacturing process of these kind of materials related to the high melting temperature and the contamination that came from atmospheric agents [33].

The figure 1 shows the main components of an EBM machine. Firstly, a layer of powder (contained in the powder hoppers) is raked over a heated building platform (For the Arcam A2X uses a stainless steel platform of dimensions 200x200mm)[34]. The thickness of the layer of powder is one of the manufacturing parameters defined by the use, in the case of titanium aluminide is usually in the range of 70 to 150µm [31][6][19][22][23].

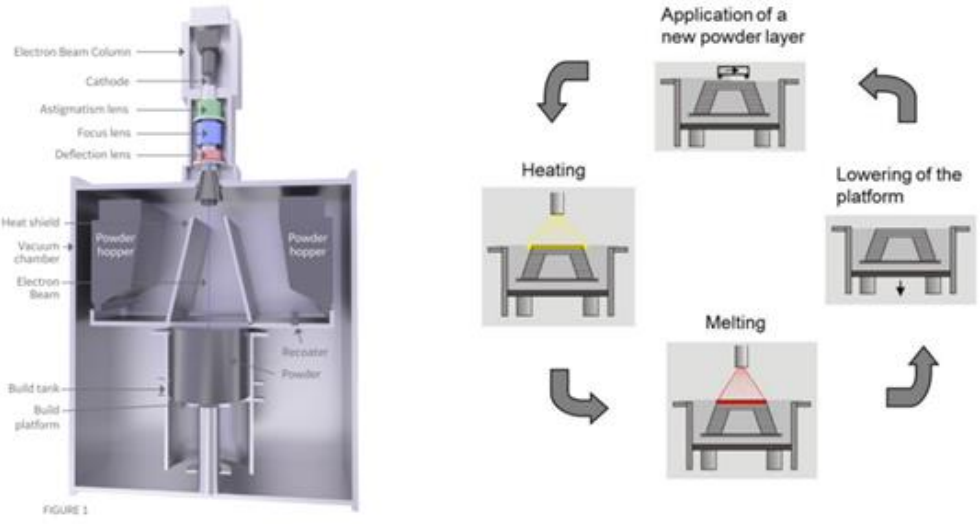

Figure 1.Schematic of EBM process [34][31]

The next step is the heating of the layer of powder. This is done using the scanning the electron beam over the layer of un-sintered powder at a high scanning speed and using a power not enough to melt the material. The preheating temperature can be set for each material, in the case of titanium aluminide materials, it should be above the ductile to brittle transformation temperature (around 800°C) [35]. Previous studies done to characterize the mechanical properties of EBM manufactured titanium aluminide samples used pre-heating temperature of 1050°C. Pre-hating the powder before the melting step allows to obtain a final component without residual stresses and cracks, compared it with laser melting fabricated ones [31].

In the melting phase, the electron beam scans the powder bed with a slower scanning velocity and higher to melt the powder material. For this operation, the beam power, scanning velocity, distance between lines, focus offset, number of contours must be defined [31]. It must be defined also the scanning strategy that can be hatching, and contour as shown in the figure 2. The normal hatching is used to create bulk melt area and contour that creates a barrier between the non-sintered powder and the hatched area[36].

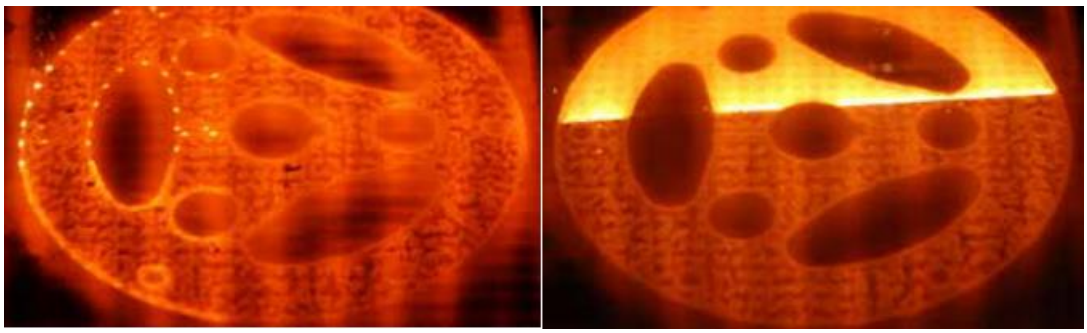

Figure 2. Scanning strategies [36].

The heat source for the melting is generated in the electron beam column by means of a cathode or a tungsten filament. The beam is controlled using three electromagnetic lenses, one to control the shape (astigmatism lens), the second controls the focus and the last one the size (deflection lens) [32]. Because this process has no movable parts, high scanning speed can be achieved (up to 8000 $^{m}/_{s}$) [34].

During the entire process, a vacuum system maintains a pressure of $5 * 10^{-5}\ mba$ inside the chamber, and during the process helium at a pressure of $4 * 10^{-3}\ mba$ to control the build environment [36]. This allows to maintain the temperature of the preheated powder to the optimal one for each material allowing to obtain the desired microstructure, obtain parts free of residual stresses and avoiding further hot post processing reducing the manufacturing cost and time. Being a hot process also allows the processability of extremely brittle and crack prone materials like titanium aluminides materials like Ti-48Al-2Cr-2Nb and Ti-47Al-2Cr-2Nb because the manufacturing process can be done above their ductile to brittle transformation temperature that is around 800° C [35]. Usually the pre-heating temperature used for this materials is above 100°C [2][6][20]. Another benefit of the use of EBM for manufacture titanium aluminides components is that a low residual stress is obtained and good apparent density can be achieved [31] [36].

After the melting phase is done, the building platform is lowered one-layer thickness, power is raked over and the preheating and melting stage are repeated for the new layer. After finishing the manufacturing process, a in situ heat treatment or high isostatic pressure (HIP) can be done to obtain finer microstructure and obtain better characteristics for the component [32][31]. Finally, the exceed of powder that remain around the final component is removed in a powder removal station that uses a similar concept as a blasting cabinet [34].

Up to now, Arcam AB Corporation, a Sweden-based company is the only manufacturer of EBM machines for industrial uses. There are some research groups that developed their own EBM machine, for academic purposes [31].

If compared whit other additive manufacturing techniques, the main advantages of using EBM technologies is that is a hot process, allowing it to maintain the temperature of the powder at temperature above 1000°C during the entire building process. This allows the processability of high temperature materials like titanium aluminides than cannot be easily processes using laser technologies[32][25].

Also, because the powder around the component is sintered, less supports are needed leading to a better stacking of the parts in the building chamber, less material is melted, the freedom for the designer is increased and less post processing time is needed to take out all the supports [34].

Regarding the microstructure and chemical composition of the samples of titanium aluminide made via EBM, aluminum loss can occur in a small amount depending on the manufacturing parameters [37]. Also the good homogeneity in the chemical composition and low defects and porosity can be achieved [37].

Another point in favor of EBM is that the production cost can be half of the ones for laser machines for some materials like aluminum alloys [36].

3.1.2. Laser Powder Bed Fusion (LPBF)

Laser powder bed fusion (LPBF) or selective laser melting (SLM) is an additive manufacturing technique that uses as raw material powder, but contrary to EBM, uses one or more than one laser as heat source [15]. Whit this technique is also possible to achieve near 100% density in the manufactured components, but usually in order to achieve optimal mechanical properties a post treatment like hot isostatic pressing (HIP) [15].

Similarly, to EBM, the process begging from a 3D cad model of the component to be manufactured. Then the build parameters are set according to the machine and the material. The component is built layer after layer by into an inert chamber by means of melting of each layer of powder using one or more laser beams at heat source. After each layer is completed, the build platform is lowered one-layer thickness in the z direction. The motion of the laser is controlled by galvanometers, resulting in a scanning speed lower than the one obtained using EBM technologies. A schematic figure of LPBF is shown in the figure 3 [38].

In comparison whit EMB, LPBF technologies present some disadvantages. First of all, the need of an additional post process to achieve similar mechanical properties for some materials, this

extra step increases in the manufacturing time and cost. Also, because of the working temperature and cannot be controlled like in the case of EBM, component manufactured using materials whit low ductility at room temperature like titanium aluminide tends to be prone to cracks [14]. An advantage of this process over EBM is that it can produce component whit higher accuracy, better surface finishing and offer more material options [39].

Some research has been done in order to characterize titanium aluminides materials characteristics using samples manufactured via LPBF. Due to the high cooling rate, cracks were founded after the solidification. Also, oxygen pick up tends to produce brittleness in the components. Regarding the mechanical properties, the obtained results were lower in comparison with samples produced using other techniques [25].

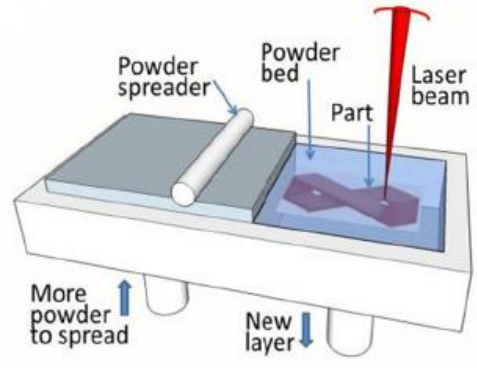

Figure 3. Schematic LPBF [38]

3.2. Directed Energy Deposition

In contrast to powder bed additive manufacturing technologies, direct energy deposition uses as raw material a metal wire or powder and as a heat source a welding arc, an electron beam or a laser beam, in order to melt the material. This techniques can be used for many metallic materials like nickel alloys, aluminum alloys and titanium base materials [13].

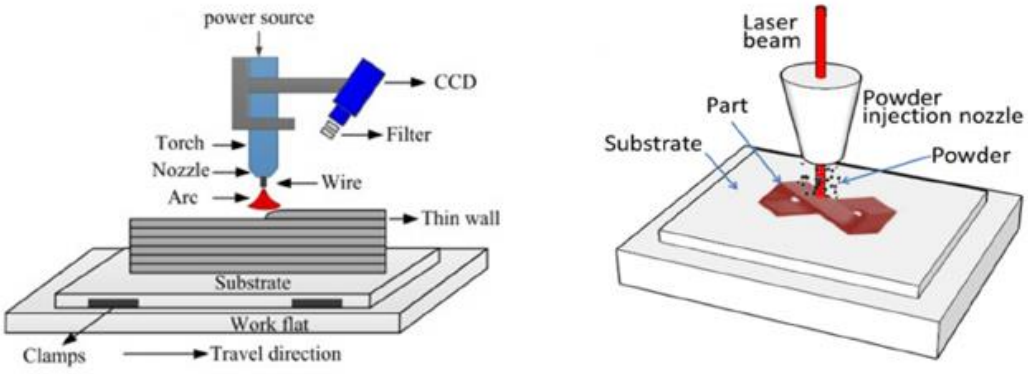

Figure 4. Schematic DED [38].

In the case of electron beam free-form (EBF) and direct laser fabrication (DLF) the metallic powder is added through an nozzle and a heat source is use to create the molten pool, additionally, a gas protection is needed in order to protect it from oxidation. For the wire arc additive manufacturing (WAAM) solution the heat source is provided by means of an electric

arc while uses metallic wire as feedstock, and likewise to the previous described methods, it also uses gas a as protection from the environment [13][38].

The lack of dimensional accuracy, the presence of defects and the poor surface finishing represent a disadvantage of DED over powder bed processes. On the other hand, an advantage of this technique over EBM and LPBF is that can be used for manufacture process and also for repair components, the maximum building dimension is usually larger, the deposition rate is higher and can offer cost saving regarding the raw material [32][38][13].

The use of direct energy deposition for titanium aluminides present a large sensitivity for crack formation and low surface finishing due to the rapid cooling rate. Also the aluminum loss in the process and the no homogeneous microstructure leads to a lower characteristics in comparison with other methods [25]

4. Experimental test on titanium aluminide bulk samples manufactured via EBM

In recent years, researchers performed experimental analyses in order to characterize the mechanical properties of titanium aluminide component manufactured using EBM technology. These studies have been done mainly on bulk samples, previously machined and focused in the comparison of the characteristics at room temperature and at elevated temperature. The following table shows the manufacturing parameters, samples dimensions and results of the mechanical test at room temperature.

Reference	Powder composition	Young Modulus [MPa]	Yield strength [MPa]	UCS [MPa]	Sample dimensions [mm]
[6]	Ti-48Al-2Nb-0.7Cr-0.3Si	166 ±2	253 ±13	336 ±2	32xø6.25
[19]	Ti-48Al-2Nb-2Cr	150, 161		754, 726	75x10x10
[20]	Ti-48Al-2Nb-2Cr		566, 605, 587		5x1.5x0.8
[21]	Ti-48Al-2Nb-2Cr		478.9 ±2.3	2526.2 ±81.9	6xø4
[40]	Ti-48Al-2Nb-2Cr		546 ±25	641 ±25	5x1.2x0.75
[23]	Ti-48Al-2Nb-2Cr		460		25xø5

Table 1. Mechanical properties test in samples made of titanium aluminide at room temperature.

Baudana et al. [6] performed tensile and creep test in specimens manufactured using Ti-48Al-2Nb-0.7Cr-0.3Si material. The samples were heat treated and then machined to reduce the surface roughness. Before the mechanical characterization, a chemical analysis has been done in which they detected a small aluminum loss (lower than 2%). The mechanical test was performed at room temperature and at 800°C.

Seifi et al. [19] analyzed the properties of cylindrical and square cross-section parallelepiped samples of Ti-48Al-2Cr-2Nb and compare them with the properties of casted titanium aluminide. They observed that in both cases, γ grain were obtained. Regarding the mechanical properties, the as-build material exceeds the properties of cast TiAl, but numerous cracks were found. On the other hand, the hiped samples showed a decrease in the number of cracks and a slight reduction in the mechanical properties.

Todai et al. [20] demonstrated that Ti-48Al-2Nb-2Cr strength an elongation differ significantly according to the loading direction in relation to the build direction of the samples. Also conclude that the anisotropy decreases as the temperature increase from room temperature up to above 700° C.

Another study that compare properties of EBM manufactured samples and compared it with plasma -melted at different temperature was carried out by Youn et al. [21]. The results shown that that the properties decrease as the temperature increases.

5. Lattice structures

In contrast to fully dense components, lattice structures, also known as cellular structure, are made by cylindrical or square cross-section parallelepiped struts connected by means of nodes. Because lattice structures shown good strength to weight ratio, good thermal dissipation, and good energy absorption, they have been used in many engineering applications. For that reason, the characterization of these structure becomes important [41]. All lattice structures can be described by its unitary cell, that is the simplest structure that is repeated through all the component. It is also necessary to describe the struts length and dimeter or sides length of the cross-section [32].

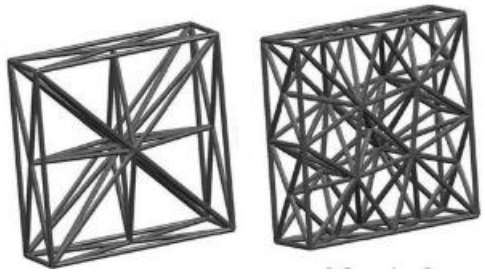

Figure 5. Mesh 1 and Mesh2 unitary cell studied by Liu et al [42].

Additive manufacturing techniques like EBM and SLS have boosted research activities about characterization of lattice structures, and because different geometries have been analyzed [17]. As shown in the figure 5, Liu et al. presented two type of meshes made of cylindric struts connected by one node in the case of Mesh 1 and by four nodes in the second case [42]. Galati el al. choose a octet-truss, unit cell made of cylindrical struts as shown in the figure 6 [43]**.** Other cylindrical struts manufacturable by AM technologies are the Kelvin and Gibson-Ashby [41]. Mohammad et al. presented a different alternative, a block structure made of square cross-section (figure 7)[22].

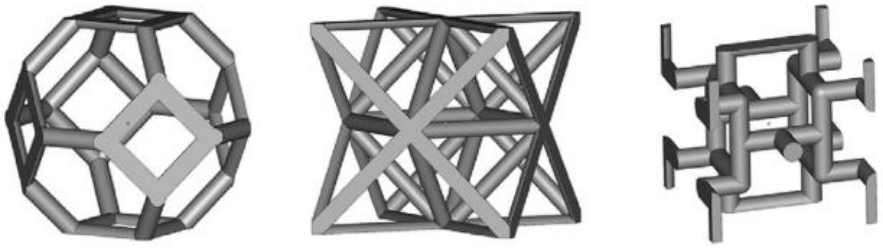

Figure 6. Kelvin, Octet-truss, and Gibson-Ashby unitary cell [43].

Figure 7. Block structure unitary cell [22].

Gibson and Ashby developed a model after a series of test in which they conclude that the mechanical properties of cellular structure are proportional to the properties of a fully dense component of the same material, and also is related to the cell topology and shape. The following two empirical equations describe an approximation of the elastic modulus and ultimate compressive strength. The start values refer to the lattice structure sample and the sub-s to the properties of a solid sample of the same material. The constant C_1 and C_2 can be obtained through experimental tests, and are unique for each material and lattice type[44] [32].

$$\frac{E^*}{E_s} = C_1 \left(\frac{\rho^*}{\rho_s}\right)^2$$

$$\frac{UCS^*}{UCS_s} = C_2 \left(\frac{\rho^*}{\rho_s}\right)^{\frac{3}{2}}$$

5.1. Mechanical properties of titanium aluminide lattice structures manufactured via EBM

Different research activities have been done in order to characterize the mechanical properties of lattice structures samples manufactured via EBM, especially the ones made of Ti-6V-4Al. In this experimental test the aim is to find the optimal manufacturing parameters (Scanning speed, scanning strategy, powder chemical composition, powder size, preheating temperature, layer thickness) to obtain samples in which the geometry do not defer significantly from the Cad model, because this can have impact in the final mechanical properties (elastic modulus, yield strength, ductility) of the component [17].

Regarding the use of titanium aluminides, the only research that can be found in the literature is the one presented by Mohammad et al. [22], in which they manufactured block structures made of Ti-48Al-2Cr-2Nb. Using different build parameters as shown in the table 2, they build block lattice structures samples, with struts sizes of 1.5mm 1mm and 0.5mm as shown in the figure7. To compare the geometry of the samples again the CAD model, the porosity was analyzed using 3D illustration obtained by a µ-CT analysis, and later compared with the 3D

model of the sample. The results showed that the internal porosity was minimal (around 0.2% for the structures of 0.5mm). In the compression tests they observed that the stress-strain curve have tree parts, one linear elastic deformation, a plateau region and a the stress hardening region as in the figure X and the values of the build parameters and mechanical properties are shown in the table 2. In concordance with the Ashby-Gibson model, the Young modulus and UTS decreases as the porosity volume of the sample increase, as can be appreciated in the figure 8.

Sample Number	Sample Conditions			Young's Modulus (GPa)	Peak Compressive Stress σ (MPa)
	Strut Size (mm)	Current (mA)	Scan Strategy		
1	1.5	18	Standard	2.39 ± 0.51	186 ± 6.22
2	1.5	12	Standard	Not tested	Not tested
3	1.5	6	Standard	2.59 ± 0.02	186 ± 0.20
4	1	18	Standard	1.46 ± 0.04	111 ± 0.07
5	1	12	Standard	1.71 ± 0.02	111 ± 1.07
6	1	6	Standard	1.35 ± 0.07	96 ± 0.71
7	0.5	18	Standard	Build failed	Build failed
8	0.5	12	Standard	Build failed	Build failed
9	0.5	6	Standard	Build failed	Build failed
10	1.5	18	Modified	2.67 ± 0.16	255 ± 5.59
13	1	18	Modified	1.91 ± 0.07	125 ± 7.76
16	0.5	18	Modified	0.81 ± 0.05	26 ± 0.33

Table 2. Mechanical properties test in samples made of titanium aluminide [22]

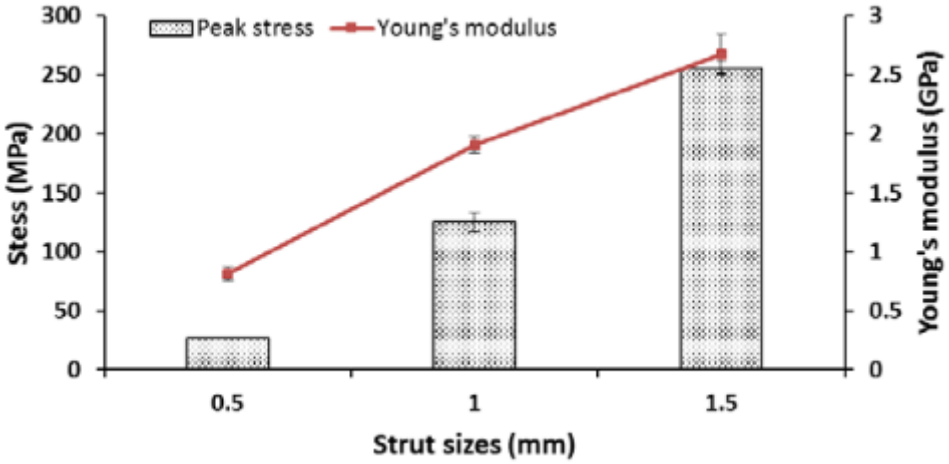

Figure 8. Comparison of mechanical properties for different struts sizes [22].

6. Experimental activities

6.1. Samples

For this study fourteen different cubic samples of 20x20x20 mm with a dodecahedron lattice structure have been produced using the software Magics 21.11. The nomenclature of the samples consists in tree parameters. First, the struts size that can be medium or thin (M or T), then the cell size expressed in millimeters after, and finally the fabrication parameters, five different strategies called NET1 to NET5.

The exacts parameters of the build strategies cannot be disclose yet because it will be used in further works and publications. There are four parameters that can be modified during the setup of the build: the scanning speed for the contour and the for the hatching, the focus of the electron beam and the current. The Table 4 presents a description of the five strategies.

For instance, the Figure 9 corresponds to the sample M5_3-NET3 have Strut size medium, with cell size equal to 5mm and fabrication was manufactured using the strategy 3.

Sample	Cell size	Strut size [mm]	Strategy
M5_2-NET1	Medium	5	NET1
M5_2-NET2	Medium	5	NET2
M5_3-NET3	Medium	5	NET3
M5_3-NET4	Medium	5	NET4
M5_4-NET5	Medium	5	NET5
T5_12-NET5	Thin	5	NET5
T5_13-NET3	Thin	5	NET3
T5_14-NET4	Thin	5	NET4
T5_22-NET1	Thin	5	NET1
T5_23-NET1	Thin	5	NET1
T5_24-NET2	Thin	5	NET2
T6_6-NET5	Thin	6	NET5
T6_11-NET3	Thin	6	NET3
T6_16-NET1	Thin	6	NET1

Table 3. Samples nomenclature.

Strategy	Scanning speed outer contour	Scanning speed inner contour	Focus offset	Beam current
NET2	low	low	high	high
NET3	low	low	high	low
NET4	high	high	high	high
NET5	high	high	low	high

Table 4. Manufacturing strategy.

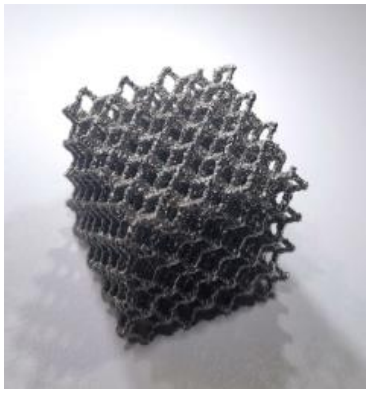

Figure 9. Sample M5_3-NET3(a). Unitary dodecahedron cell [45]*(b).*

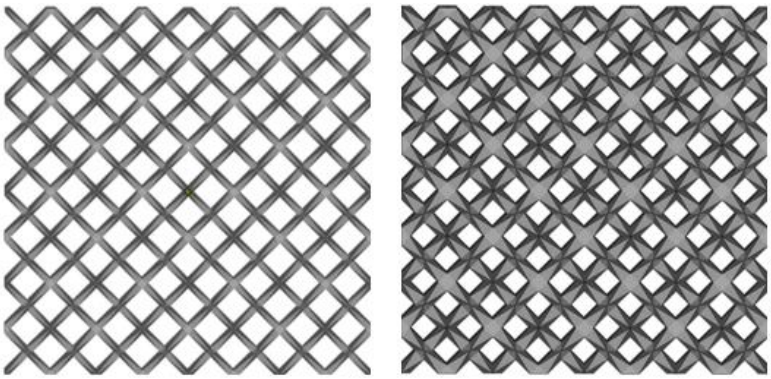

Figure 10. Thin and Medium struts size

6.2. Production and verification

The samples were build using an Arcam A2X EBM machine with Ti-64Al-2Cr-2Nb using the EBM build processor 5.0 with a Ti-64Al-2Cr-2Nb Standard Theme for the Arcam A2X system The samples were not produced directly on the build plate, but rather a bulk support structure of 30mm have been built between the plate and the lattice structure. The samples where oriented at the same level and tilted 45 degrees as can be observed in the Figure 11. After the build has finished, the samples have been cooled down inside the build chamber up to room temperature, before being blasted in a powder recovery system using TiAl powder and then cleaned using compressed air.

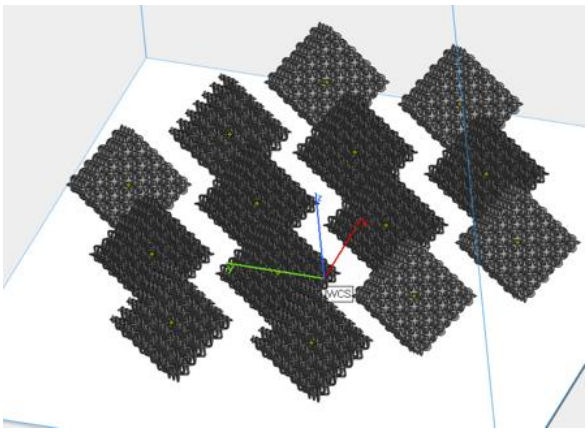

Figure 11. Samples orientation

In order to verify that the structs were correctly built, images of all samples were capture using a Leica microscope at 0x, 1x and 2x magnification. An example of this image is shown in the figure 12. The procedure was repeated for all samples and no defective samples were found.

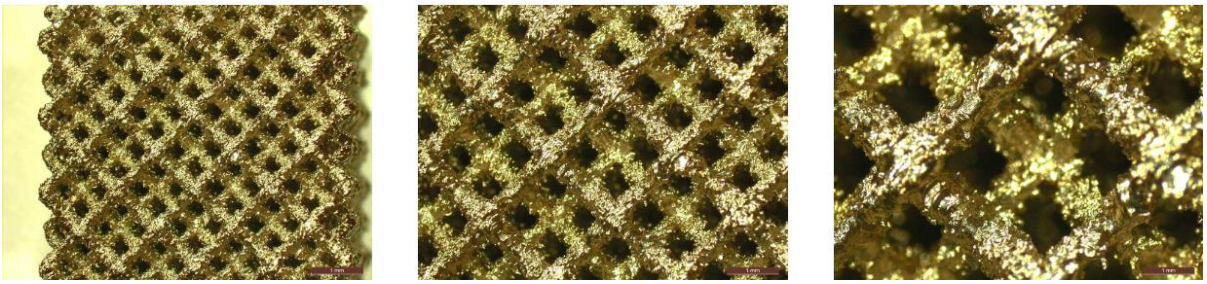

Figure 12. M5_2-NET1 sample a 0x, 1x and 2x.

To determine the presence of porosity in one face of the sample, a porosity analysis was carried out as follow: first the samples were polished using sandpapers of 600, 800 and 1200 and diamond powder of3 µm and1 µm, after this process was completed, the samples were cleaned and then by means of a S9i microscope, images at 50x magnification were collected. For each sample four to six image from the nodes on the polished face were collected and analyzed. The analysis consisted in estimate the surface area corresponded to the lattice structure and the area of the porosity founded in each one using the image histogram function of MATLAB and the scale obtained from the Leica post processing software.

The results demonstrate as can be seen in the table below show that the samples were produced free of significant porosity. The highest result is 99.11% for the samples M5_4-NET5 and T6_11-NET6, while the lower corresponds to the sample T6_11-NET5 whit 96.97%.

Sample	Average [%]
M5_2-NET1	98.72
M5_2-NET2	98.82
M5_3-NET3	98.54
M5_3-NET4	99.08
M5_4-NET5	99.11
T5_12-NET5	98.22
T5_13-NET3	98.83
T5_14-NET4	99.00
T5_22-NET1	98.21
T5_23-NET1	98.73
T5_24-NET2	98.02
T6_6-NET5	96.97
T6_11-NET3	99.11
T6_16-NET1	98.47

Table 5. Percentage free of porosity of the cross-section area.

6.3. Compression test

6.3.1. Test Description

The compression test was carried out using a Easydur 3Mz universal testing machine using Ti6V4Al plates as shown in the Figure 13 to avoid denting the plates with samples that could lead to a misreading of the actual displacement. For the data acquisition was used the EasyQS software whit an acquisition rate of 50 Hz saving the parameter of the load and displacement.

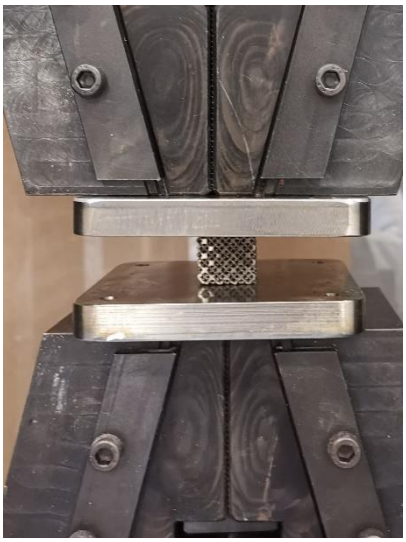

Figure 13. Sample before compression.

A strain-controlled test was performed at a constant displacement rate of 2 $^{mm}/_{min}$ until the failure of the samples.

From the data collected, it was calculated the strain and stress for each sample using the following formulas.

$\sigma = \frac{P}{A}$ and $\varepsilon = \frac{\delta}{l_o}$

Where P is the load, δ the displacement, A the area of a square of 20mm and $l_o$the initial length equal to 20mm.

To evaluate the compressive Young modulus, 4 points were chosen along the linear part of the curve and computed the Young modulus of the segment, then the average was computed as the Young modulus of the sample.

$$E_1 = \frac{\sigma_{f2} - \sigma_{f1}}{\varepsilon_{f2} - \varepsilon_{f1}}$$

6.3.2. Failure mechanism

In all samples a brittle behavior was observed. The samples collapsed into two pieces at an angle close to 45 degrees, into multiple small pieces, or into wedge-shaped pieces and the

load decreases immediately. The following table shows the description of the failure of each sample.

Sample	Failure mechanism
M5_2-NET1	Two pieces at 45 degrees
M5_2-NET2	Several small pieces
M5_3-NET3	Two pieces at 45 degrees
M5_3-NET4	Two pieces at 45 degrees
M5_4-NET5	Several small pieces
T5_12-NET5	Two pieces at 45 degrees
T5_13-NET3	Several small pieces
T5_14-NET4	Several small pieces
T5_22-NET1	Several small pieces
T5_23-NET1	Several small pieces
T5_24-NET2	Several small pieces
T6_6-NET5	Two pieces at 45 degrees
T6_11-NET3	Two pieces at 45 degrees
T6_16-NET1	Several small pieces

Table 6. Failure mechanism.

Figure 14. Failure of the sample M5_2-NET1 (a). Failure of the sample M5_2-NET2 (b).

6.3.3. Compressive trends

In all samples a brittle behavior was observed that a first large elongation where registered without an increase in the load, and after that the load increases linearly until the fracture al the UTS point as shown in the figure 14.A. This first deformation is caused by the deformation of the tips of the nodes in the upper and lower face of the sample. Another factor that contributes is that the faces are not perfectly flat, in fact part of this initial deformation occurs also in the setup process of the test. For that reason, the data were post processed and that initial part was excluded of the analysis. The results are displayed in the Table 6. Regarding

the repeatability, the samples T5_22net1 and T5_23net1 have the same geometry and manufacturing parameters. The obtained results differ only in 5% for the UTS and 1.6% for the Young modulus as can be appreciated in the Figure 15. Is also worth to mention that the sample T5_13-NET3 exhibit a result that is extremely lower in comparison with the other samples. This can be consequence of a defect in the manufacturing process.

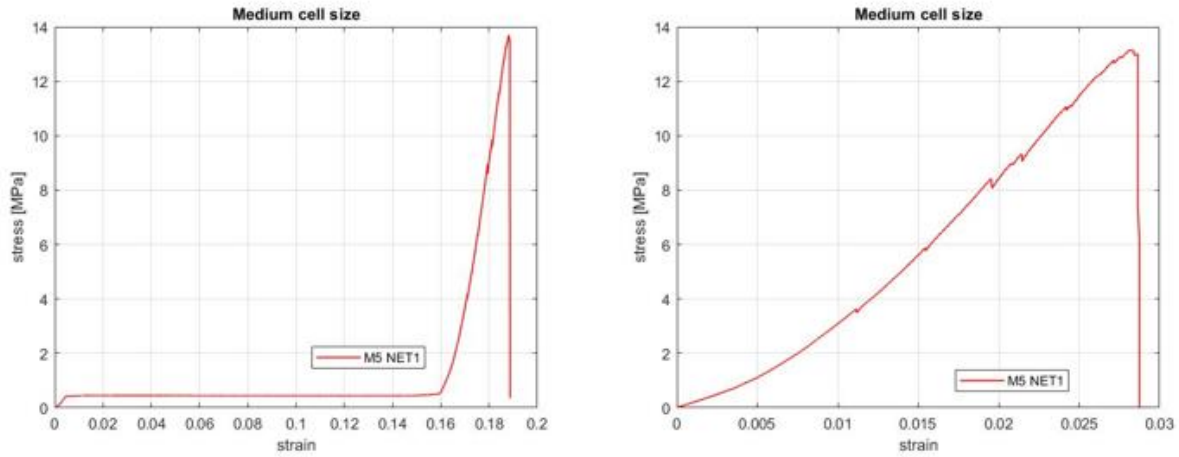

Figure 15. Strain-stress plot before post-processing (a). Strain-stress plot after post-processing (b)

Sample	UTS [MPa]	E [MPa]
M5_2-NET1	13.15	428.70
M5_2-NET2	8.24	297.89
M5_3-NET3	7.02	351.15
M5_3-NET4	8.54	299.12
M5_4-NET5	11.24	421.15
T5_12-NET5	2.26	97.12
T5_13-NET3	1.13	4.59
T5_14-NET4	2.60	141.28
T5_22-NET1	2.95	168.81
T5_23-NET1	2.81	171.55
T5_24-NET2	2.65	177.20
T6_6-NET5	1.98	130.99
T6_11-NET3	0.91	54.61
T6_16-NET1	0.94	118.36

Table 7. Value of Ultimate tensile stress and Young Modulus.

6.3.4. Repeatability

Regarding the repeatability, the samples T5_22net1 and T5_23net1 have been manufacturer using the same lattice geometry and building strategy. The results of the mechanical properties obtained for this pair of samples differ from each other only in 5% for the ultimate tensile strength and 1.6% for the Young modulus as can be appreciated in the Figure 16.

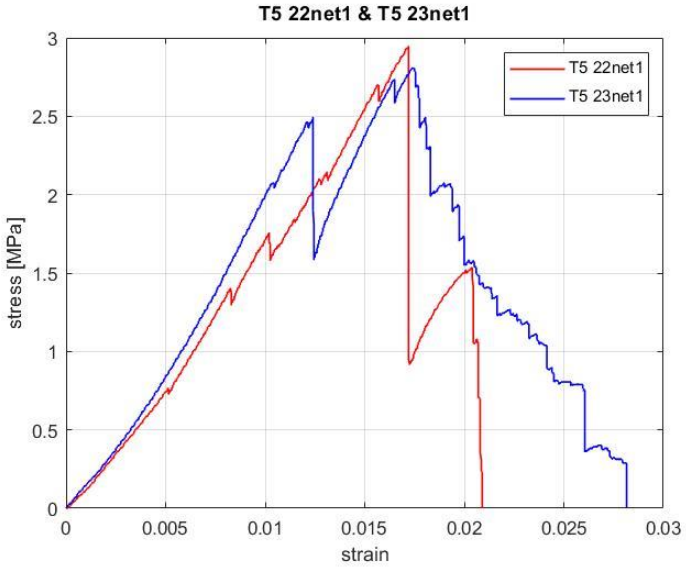

Figure 16.Comparison of the results of sample T5_22net1 and T5_23net1

6.3.5. Influence of the cell size

Samples manufactured with five building strategies were tested. For the strategies NET1 and NET 5 there were samples with three different lattice geometry, and for the strategies NET2, Net 3, Net 4 there were samples with two different lattice geometries.

From the data in Figure 17, can be conclude that the cell size have is an important factor in the behavior of this samples. For the five different strategies the samples with medium cell outperform the ones with thin by a large margin. For instance, in for the strategy NET1, the difference of the UTS value of M5_2-NET1 respect to the samples with cell size T5 and T6 are 357 and 1029 % respectively. For the Young modulus also the difference is significant, 150% with T5 and 1437% for T6.

This trend is repeated whit the other four strategies, in which the difference between the values for the M5 samples with respect to the T5 ranges from 211% to 398% for the UTS and 68% to 330% for the Young modulus. With T6, the difference is even bigger with differences that rages ranges from 467% to 667% for the UTS and 221% to 542% for the Young modulus.

This results correlates with the Ashby-Gibson model [44] described in the chapter 5.1 . It exposes that the mechanical properties of solid foams are related to the mechanical properties of the bulk sample made of the same material and the porosity of the study samples.

In this case, the samples with cell geometry T6 will corresponds to a higher level of porosity, the sample T5 and finally M5. To correctly compute the values as presented in the chapter 5.1 it will be necessary also to manufacture bulk samples with each build strategy to obtain the value of UTS and Young modulus and have at least 4 different geometries to have a more representative result. In this case, because of the previously mentioned the value of the constant of the equation X will not be computed.

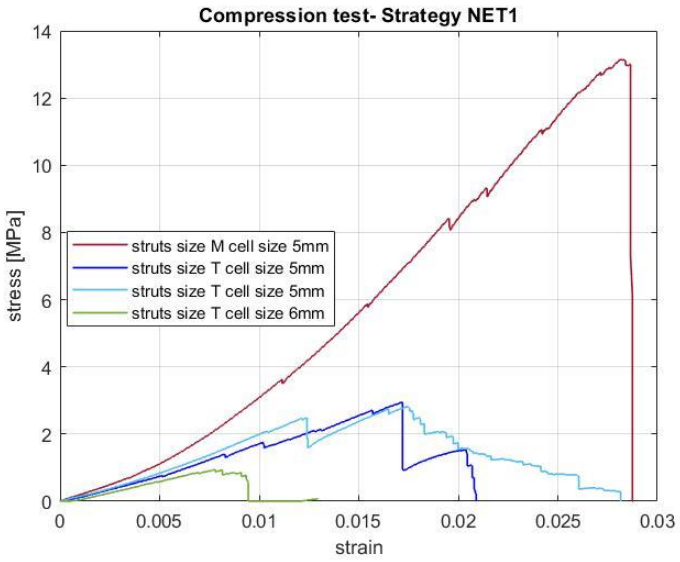
Compression test- Strategy NET1
stress [MPa]
strain
struts size M cell size 5mm
struts size T cell size 5mm
struts size T cell size 5mm
struts size T cell size 6mm

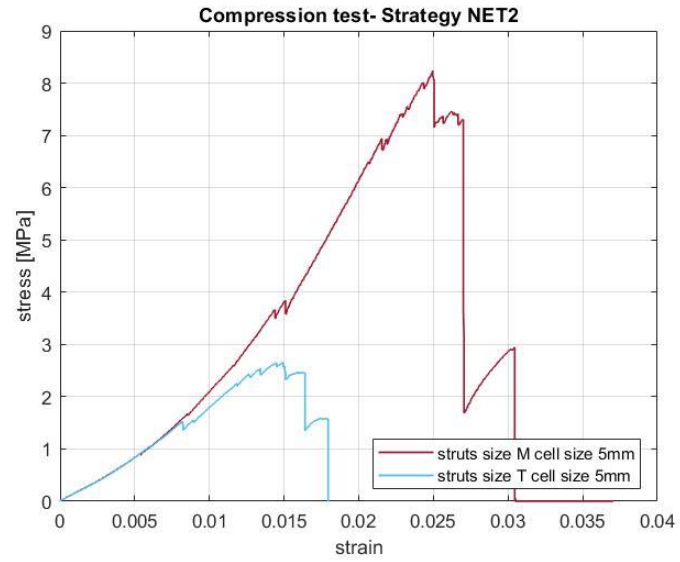
Compression test- Strategy NET2
stress [MPa]
strain
struts size M cell size 5mm
struts size T cell size 5mm

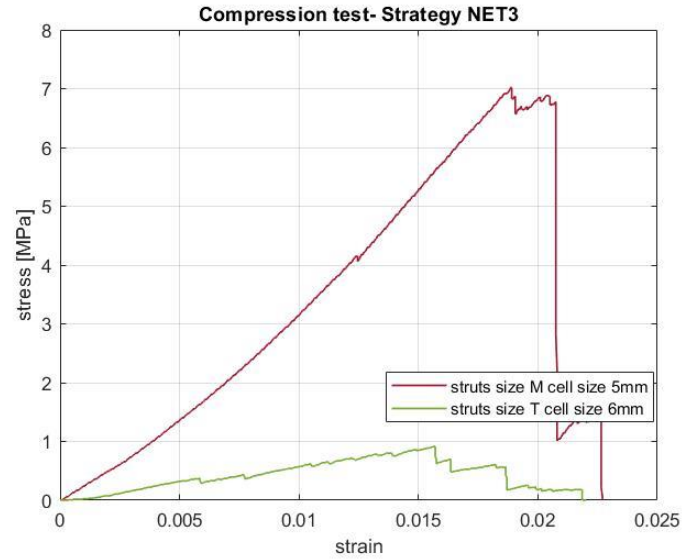
Compression test- Strategy NET3
stress [MPa]
strain
struts size M cell size 5mm
struts size T cell size 6mm

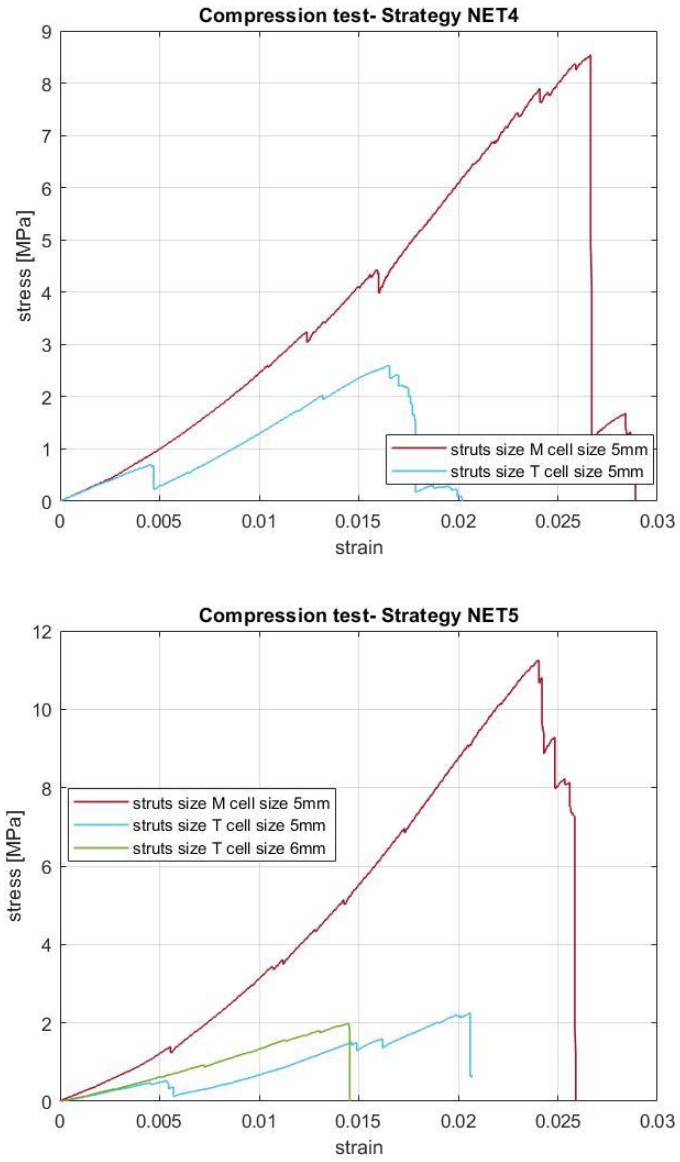

Figure 17. Stress-strain plot Strategy Net1(a), Stress-strain plot Strategy Net2(b), Stress-strain plot Strategy Net3(c), Stress-strain plot Strategy Net4 (d), Stress-strain plot Strategy Net5(e).

6.3.6. Influence of the manufacturing strategy

In other to analyze the influence of the manufacturing parameters, the Figure 18 shows the trend for samples with similar geometry but five different build strategies.

In the Figure 18.a that corresponds to the samples whit Medium struts size the samples manufactured using the strategies NET1 and Net5 have similar performances. For instance, the Young modulus are 429MPa and 421 MPa respectively, and the UTS 13.15MPa and 11.24 MPa. For the samples NET2, NET3 and NET4 the values range from 7.02 MPa to 8.54MPa for the UTS range from 298MPa to 351MPa.

The strategy NET1 is also the one that have better performance between the samples with cell geometry T6 with a UTS of 2.95MPa and UTS 169MPa, but the samples NET5 ais the one with lower results.

On the other hand, among the samples whit thin struts and cell size 6mm, the sample NET5 outperform the other two samples (NET1 and NET3) with a UTS that is almost double of the other two and an young modulus that is three times bigger.

In summary, these results show that for each lattice geometry there is and that is not necessarily the same for all.

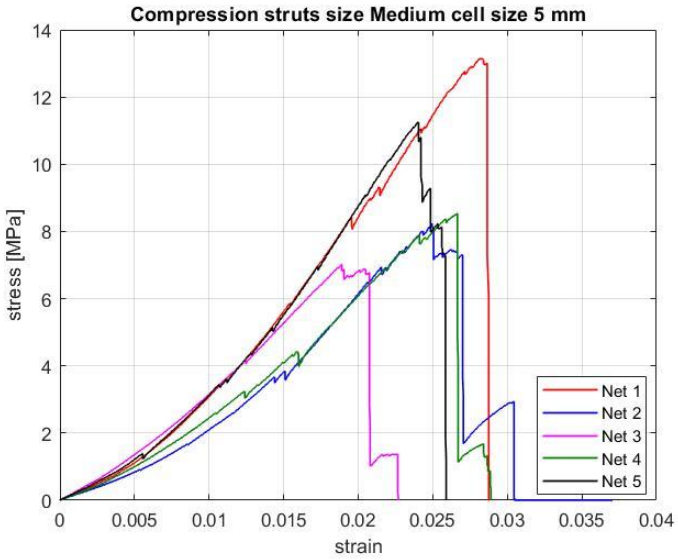

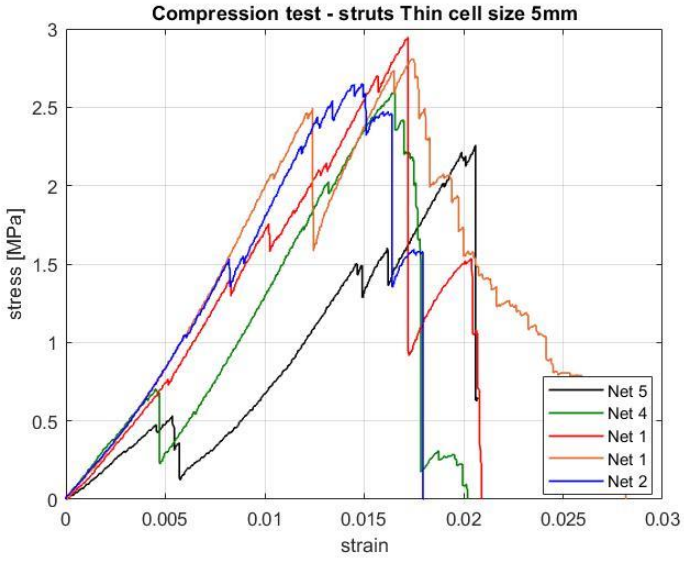

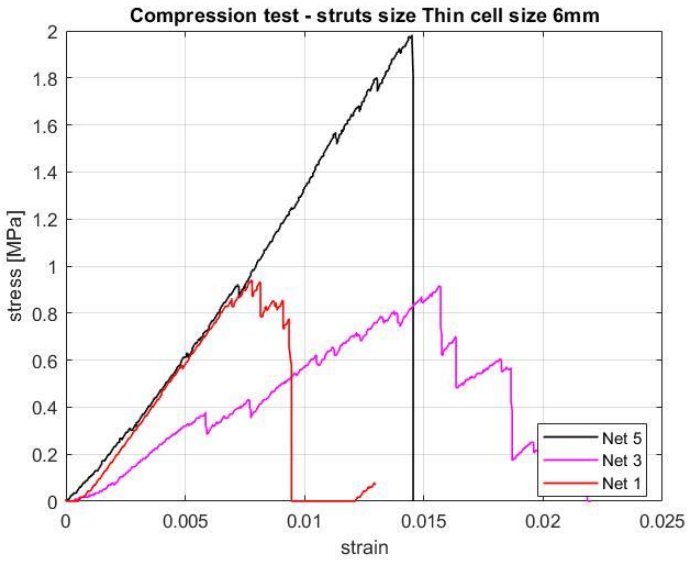

Figure 18. Stress - strain plot for the samples with lattice M5 (a). Stress - strain plot for the samples with lattice T5 (b). Stress - strain plot for the samples with lattice T6 (c).

6.4. Correlation with the Gibson-Ashby model

As mentioned in previous chapter, the exact values of the constants of the Gibson-Ashby model will not be computed in this work. To describe if the obtained values correlate with this theory, it is possible to plot the results of the samples manufactured with the three cell geometries and the same build strategy. In this case it is possible to plot for the samples NET1 and Net5. In the figure 19 can be observed that the results for the strategy NET5 do not agree with the model because the properties of the T5 are lower t than the ones of the T6 that have higher porosity. In the case of the samples NET1 the results agree with the model. In any case, as mentioned in the chapter 6.3.6, the mechanical properties seem to be affected not only from the strategy, but rather from the combination of strategy and geometry.

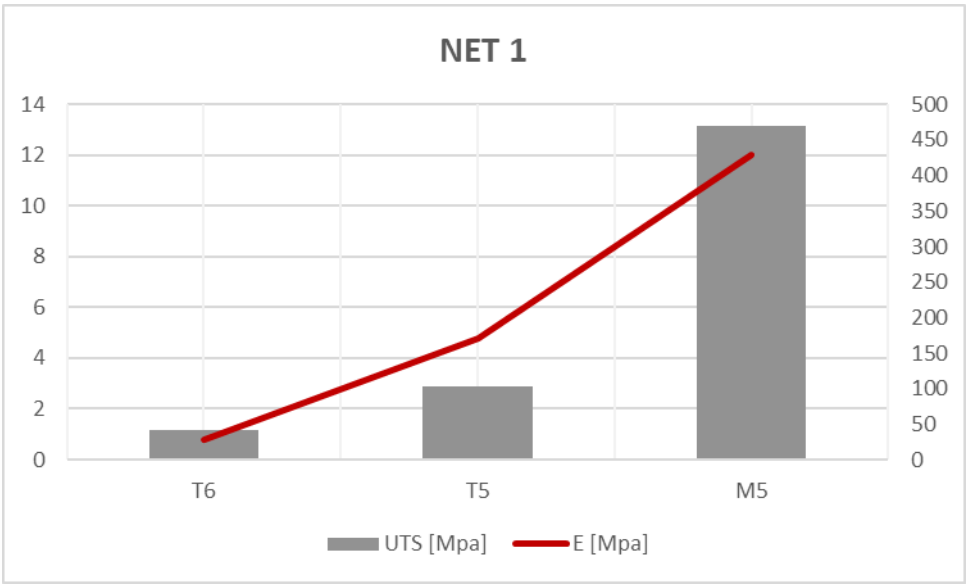

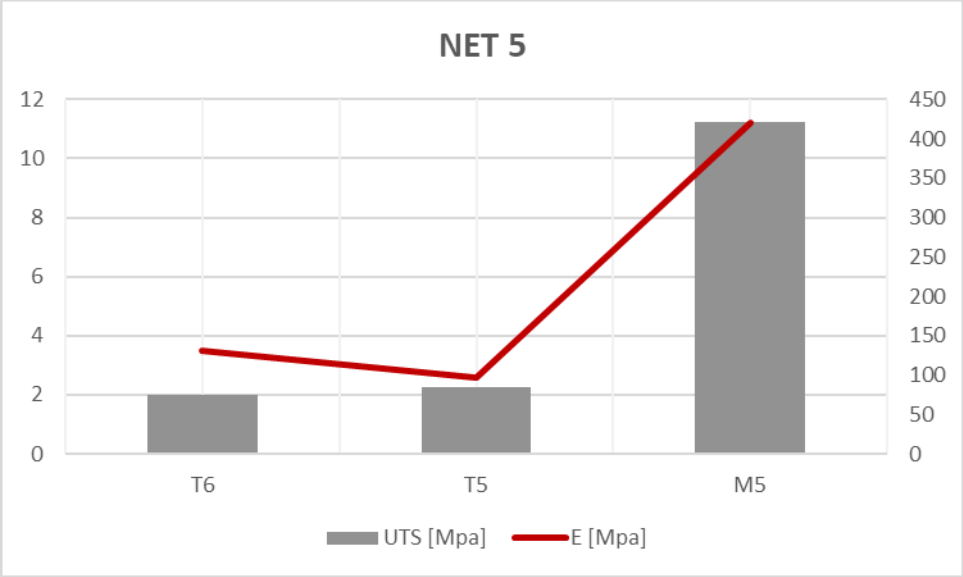

Figure 19. UTS and Young modulus for samples with build strategy NET 1(a). UTS and Young modulus for samples with build strategy NET 5 (b)

7. Conclusions and Recommendations

In this work the manufacturability and properties of titanium aluminide lattice structures components manufactured by electron beam melting have been studied. First of all, a state of the art review have been done. It was notice that previous works in this field focused more on the use of others titanium base materials like the Ti-6Al-4V. Also, the use of traditionally manufactured titanium aluminide components is concentrated only for specific applications, and because of that there is not a great number of papers regarding this topic.

From the review and experimental test, the following conclusions can be written:

1- Among the technologies available in the market, Electron Beam Melting is the most suitable option for the manufacture of titanium aluminide components because the build process take place in a controlled environment at elevated temperature reducing the formation of cracks and residual stresses in the component.
2- The EBM process is adequate for the manufacture of lattice structure components with cell size of 5mm with accuracy and good surface finishing.
3- The samples were produced without significant amount of internal porosity.
4- The data suggests that the process present a good repeatability, as expressed in the chapter 6.3.2.
5- As expected, the failure of the components has a brittle behavior. The supported load decreases rapidly after the UTS is reached.
6- The combination of the manufacturing parameters and the geometry of the lattice have an impact in the final mechanical properties of the samples. Among this two, the cell size is the one that have a greater influence.

Further works on this topic could focus on the characterization of samples using only one build strategy but with different cell size to better analyze the behavior of this material according to the Gibson-Ashby model. In addition to that, the samples could be built with two caps, one in the top and one in the bottom to avoid the problems during the setup of the compression test as described in the section 6.3.3

8. References

[1] A. Bose, “Intermetallic Compounds,” *Adv. Part. Mater.*, pp. 214–271, 1995.

[2] L. E. Murr *et al.*, “Characterization of titanium aluminide alloy components fabricated by additive manufacturing using electron beam melting,” *Acta Mater.*, vol. 58, no. 5, pp. 1887–1894, 2010.

[3] “The GEnx Engine | GE Aviation.” [Online]. Available: https://www.geaviation.com/commercial/engines/genx-engine. [Accessed: 14-Aug-2020].

[4] R. R. Boyer, “An overview on the use of titanium in the aerospace industry,” *Mater. Sci. Eng. A*, vol. 213, no. 1–2, pp. 103–114, 1996.

[5] T. Tetsui, “Development of a second generation TiAl turbocharger,” *Mater. Sci. Forum*, vol. 561–565, no. PART 1, pp. 379–382, 2007.

[6] G. Baudana *et al.*, “Electron Beam Melting of Ti-48Al-2Nb-0.7Cr-0.3Si: Feasibility investigation,” *Intermetallics*, vol. 73, pp. 43–49, 2016.

[7] G. Baudana *et al.*, “Titanium aluminides for aerospace and automotive applications processed by Electron Beam Melting: Contribution of Politecnico di Torino,” *Met. Powder Rep.*, vol. 71, no. 3, pp. 193–199, 2016.

[8] P. Santiago-Medina, P. A. Sundaram, and N. Diffoot-Carlo, “The effects of micro arc oxidation of gamma titanium aluminide surfaces on osteoblast adhesion and differentiation,” *J. Mater. Sci. Mater. Med.*, vol. 25, no. 6, pp. 1577–1587, 2014.

[9] A. Mohammad *et al.*, “In vitro wear, corrosion and biocompatibility of electron beam melted γ-TiAl,” *Mater. Des.*, vol. 133, pp. 186–194, 2017.

[10] S. A. Bello, I. De Jesús-Maldonado, E. Rosim-Fachini, P. A. Sundaram, and N. Diffoot-Carlo, “In vitro evaluation of human osteoblast adhesion to a thermally oxidized γ-TiAl intermetallic alloy of composition Ti-48Al-2Cr-2Nb (at.%),” *J. Mater. Sci. Mater. Med.*, vol. 21, no. 5, pp. 1739–1750, 2010.

[11] D. F. Castañeda-Muñoz, P. A. Sundaram, and N. Ramírez, “Bone tissue reaction to Ti-48Al-2Cr-2Nb (at.%) in a rodent model: A preliminary SEM study,” *J. Mater. Sci. Mater. Med.*, vol. 18, no. 7, pp. 1433–1438, 2007.

[12] K. Kothari, R. Radhakrishnan, and N. M. Wereley, “Advances in gamma titanium aluminides and their manufacturing techniques,” *Prog. Aerosp. Sci.*, vol. 55, pp. 1–16, 2012.

[13] X. Cai, B. Dong, X. Yin, S. Lin, C. Fan, and C. Yang, “Wire arc additive manufacturing of titanium aluminide alloys using two-wire TOP-TIG welding: Processing, microstructures, and mechanical properties,” *Addit. Manuf.*, vol. 35, no. May, p. 101344, 2020.

[14] M. Reith, M. Franke, M. Schloffer, and C. Körner, “Processing 4th generation titanium aluminides via electron beam based additive manufacturing – characterization of microstructure and mechanical properties,” *Materialia*, p. 100902, 2020.

[15] K. O. Abdulrahman, E. T. Akinlabi, R. M. Mahamood, S. Pityana, and M. Tlotleng, “Laser metal deposition of titanium aluminide composites: A review,” *Mater. Today Proc.*, vol. 5, no. 9, pp. 19738–19746, 2018.

[16] ASTM International, “F2792-12a - Standard Terminology for Additive Manufacturing Technologies,” *Rapid Manuf. Assoc.*, pp. 10–12, 2013.

[17] L. Salvo, G. Martin, M. Suard, A. Marmottant, R. Dendievel, and J. J. Blandin, “Processing and structures of solids foams,” *Comptes Rendus Phys.*, vol. 15, no. 8–9, pp. 662–673, 2014.

[18] W. Ge, C. Guo, and F. Lin, “Effect of process parameters on microstructure of TiAl alloy produced by electron beam selective melting,” *Procedia Eng.*, vol. 81, no. October, pp. 1192–1197, 2014.

[19] M. Seifi, A. A. Salem, D. P. Satko, U. Ackelid, S. L. Semiatin, and J. J. Lewandowski, “Effects of HIP on microstructural heterogeneity, defect distribution and mechanical properties of additively manufactured EBM Ti-48Al-2Cr-2Nb,” *J. Alloys Compd.*, vol. 729, pp. 1118–1135, 2017.

[20] M. Todai *et al.*, “Effect of building direction on the microstructure and tensile properties of Ti-48Al-2Cr-2Nb alloy additively manufactured by electron beam melting,” *Addit. Manuf.*, vol. 13, pp. 61–70, 2017.

[21] S. J. Youn, Y. K. Kim, S. W. Kim, and K. A. Lee, “Elevated temperature compressive deformation behaviors of γ-TiAl-based Ti–48Al–2Cr–2Nb alloy additively manufactured by electron beam melting,” *Intermetallics*, vol. 124, no. June, p. 106859, 2020.

[22] A. Mohammad, A. M. Alahmari, K. Moiduddin, M. K. Mohammed, A. Alomar, and R. K. Renganayagalu, “Porous γ-TiAl structures fabricated by electron beam melting process,” *Metals (Basel).*, vol. 6, no. 1, 2016.

[23] B. Lin, W. Chen, Y. Yang, F. Wu, and Z. Li, “Anisotropy of microstructure and tensile properties of Ti–48Al–2Cr–2Nb fabricated by electron beam melting,” *J. Alloys Compd.*, vol. 830, p. 154684, 2020.

[24] V. H. Benninghoff, T. Rundschau, F. Application, and P. Data, “United States Patent (19),” no. 19, pp. 11–14, 1994.

[25] W. Chen and Z. Li, “11 - Additive manufacturing of titanium aluminides,” in *Additive Manufacturing for the Aerospace Industry*, F. Froes and R. Boyer, Eds. Elsevier, 2019, pp. 235–263.

[26] “The Blade Runners: This Factory Is 3D Printing Turbine Parts For The World’s Largest Jet Engine | GE News.” [Online]. Available: https://www.ge.com/news/reports/future-manufacturing-take-look-inside-factory-3d-printing-jet-engine-parts. [Accessed: 14-Aug-2020].

[27] B. C. Costa, C. K. Tokuhara, L. A. Rocha, R. C. Oliveira, P. N. Lisboa-Filho, and J. Costa Pessoa, “Vanadium ionic species from degradation of Ti-6Al-4V metallic implants: In vitro cytotoxicity and speciation evaluation,” *Mater. Sci. Eng. C*, vol. 96, no. October 2018, pp. 730–739, 2019.

[28] C. Zhang *et al.*, “Mechanical behavior of a titanium alloy scaffold mimicking trabecular structure,” *J. Orthop. Surg. Res.*, vol. 15, no. 1, pp. 1–11, 2020.

[29] L. Settineri, P. C. Priarone, M. Arft, D. Lung, and T. Stoyanov, “An evaluative approach to correlate machinability, microstructures, and material properties of gamma titanium aluminides,” *CIRP Ann. - Manuf. Technol.*, vol. 63, no. 1, pp. 57–60, 2014.

[30] V. Tebaldo and M. G. Faga, “Influence of the heat treatment on the microstructure and machinability of titanium aluminides produced by electron beam melting,” *J. Mater. Process. Technol.*, vol. 244, pp. 289–303, 2017.

[31] C. Körner, “Additive manufacturing of metallic components by selective electron beam melting - A review,” *Int. Mater. Rev.*, vol. 61, no. 5, pp. 361–377, 2016.

[32] G. Del Guercio, M. Galati, A. Saboori, P. Fino, and L. Iuliano, “Microstructure and Mechanical Performance of Ti–6Al–4V Lattice Structures Manufactured via Electron Beam Melting (EBM): A Review,” *Acta Metall. Sin. (English Lett.*, vol. 33, no. 2, pp. 183–203, 2020.

[33] M. Galati and L. Iuliano, “A literature review of powder-based electron beam melting focusing on numerical simulations,” *Addit. Manuf.*, vol. 19, pp. 1–20, 2018.

[34] “Arcam EBM A2X,” p. 2.

[35] W. Kan, B. Chen, C. Jin, H. Peng, and J. Lin, “Microstructure and mechanical properties of a high Nb-TiAl alloy fabricated by electron beam melting,” *Mater. Des.*, vol. 160, pp. 611–623, 2018.

[36] GE Additive, “Electron beam melting,” *Adv. Mater. Process.*, vol. 165, no. 3, pp. 45–46, 2007.

[37] S. Biamino *et al.*, “Electron beam melting of Ti-48Al-2Cr-2Nb alloy: Microstructure and mechanical properties investigation,” *Intermetallics*, vol. 19, no. 6, pp. 776–781, 2011.

[38] T. DebRoy *et al.*, “Additive manufacturing of metallic components – Process, structure and properties,” *Prog. Mater. Sci.*, vol. 92, pp. 112–224, 2018.

[39] W. Li *et al.*, “Effect of laser scanning speed on a Ti-45Al-2Cr-5Nb alloy processed by selective laser melting: Microstructure, phase and mechanical properties,” *J. Alloys Compd.*, vol. 688, pp. 626–636, 2016.

[40] E. Cakmak *et al.*, “A comprehensive study on the fabrication and characterization of Ti–48Al–2Cr–2Nb preforms manufactured using electron beam melting,” *Materialia*, vol. 6, no. March, p. 100284, 2019.

[41] O. Al-Ketan, R. Rowshan, and R. K. Abu Al-Rub, “Topology-mechanical property relationship of 3D printed strut, skeletal, and sheet based periodic metallic cellular materials,” *Addit. Manuf.*, vol. 19, pp. 167–183, 2018.

[42] Z. Liu, M. Qi, X. Qin, D. Huang, X. Zhang, and X. Yan, “Compressive Properties of Electron Beam Melted Ti–6Al–4V Porous Meshes with Different Struts Distributions,” *Met. Mater. Int.*, vol. 26, no. 7, pp. 1060–1069, 2020.

[43] M. Galati *et al.*, “Ti-6Al-4V lattice structures produced by EBM: Heat treatment and mechanical properties,” *Procedia CIRP*, vol. 88, pp. 411–416, 2020.

[44] L. J. Gibson and M. F. Ashby, *Cellular Solids*. Cambridge University Press, 1997.

[45] L. E. Murr, “Additive manufacturing of biomedical devices: an overview,” *Mater. Technol.*, vol. 33, no. 1, pp. 57–70, 2018.